

Article

# Numerical Investigation of Supersonic Flow over a Wedge by Solving 2D Euler Equations Utilizing the Steger–Warming Flux Vector Splitting (FVS) Scheme

Mitch Wolff <sup>1</sup>, Hashim H. Abada <sup>2,\*</sup>  and Hussein Awad Kurdi Saad <sup>3</sup><sup>1</sup> Mechanical & Materials Engineering Department, Wright State University, Dayton, OH 45435-0001, USA<sup>2</sup> Mechanical Engineering Department, Al-Kufa Technical Institute, Al-Furat Al-Awsat Technical University (ATU), Kufa 54003, Iraq<sup>3</sup> Power/Mechanical Engineering Department, Engineering Technical College of Al-Najaf, Al-Furat Al-Awsat Technical University (ATU), Al-Najaf 54001, Iraq; husseinawad@atu.edu.iq

\* Correspondence: abada.2@atu.edu.iq; Tel.: +964-7714406274

**Abstract:** Supersonic flow over a half-angle wedge ( $\theta = 15^\circ$ ) with an upstream Mach number of 2.0 was investigated using 2D Euler equations where sea level conditions were considered. The investigation employed the Steger–Warming flux vector splitting (FVS) method executed in MATLAB 9.13.0 (R2022b) software. The study involved a meticulous comparison between theoretical calculations and numerical results. Particularly, the research emphasized the angle of oblique shock and downstream flow properties. A substantial iteration count of 2000 iteratively refined the outcomes, underscoring the role of advanced computational resources. Validation and comparative assessment were conducted to elucidate the superiority of the Steger–Warming flux vector splitting (FVS) scheme over existing methodologies. This research serves as a link between theoretical rigor and practical applications in high-speed aerospace design, enhancing the efficiency of aircraft components.

**Keywords:** supersonic flow; half-angle wedge; 2D Euler equations; oblique shock wave; Steger–Warming method

**MSC:** 76J20

**Citation:** Wolff, M.; Abada, H.H.; Saad, H.A.K. Numerical Investigation of Supersonic Flow over a Wedge by Solving 2D Euler Equations Utilizing the Steger–Warming Flux Vector Splitting (FVS) Scheme. *Mathematics* **2024**, *12*, 1282. <https://doi.org/10.3390/math12091282>

Academic Editor: Lihao Zhao

Received: 12 March 2024

Revised: 17 April 2024

Accepted: 22 April 2024

Published: 24 April 2024



**Copyright:** © 2024 by the authors. Licensee MDPI, Basel, Switzerland. This article is an open access article distributed under the terms and conditions of the Creative Commons Attribution (CC BY) license (<https://creativecommons.org/licenses/by/4.0/>).

## 1. Introduction

Supersonic flows over aerodynamic shapes, such as wedges, play a pivotal role in modern aerospace engineering and aerodynamics. Understanding the complex flow patterns, shock wave interactions, and aerodynamic performance associated with these configurations is essential for the design and analysis of high-speed aircraft (e.g., electrical aircraft [1]) and space vehicles. The study of supersonic flow over wedges has far-reaching implications, from military applications to the development of future-generation hypersonic vehicles [2,3].

In the pursuit of aerospace engineering excellence, the investigation of the two-dimensional, compressible, adiabatic, inviscid flow of ideal gases stands at the heart of understanding fluid dynamics under extreme conditions [4]. Within the realm of fluid dynamics, this investigation offers an opportunity into the behavior of gases at high speeds, where the very essence of flight takes shape [5]. This project embarks on a journey into this intricate domain, where it explores the dynamics of compressible flows in the absence of external forces, no heat transfer, no viscosity, and the assumption of a calorically perfect gas [6,7].

The focus centers on the interaction of supersonic flow with a geometric wedge, a configuration emblematic of numerous aerospace and aerodynamic applications, such as aircraft wings, fan blades, etc. [8]. As supersonic flow impinges upon the wedge's leading

edge; it instigates a transformative incident, the creation of an oblique shock wave at the vertex of the wedge [3], as shown in Figure 1. This shock wave, a manifestation of the fundamental principles governing compressible flows, leads to a cascade of intricate phenomena, from compression and heating to the alteration of flow properties [9].

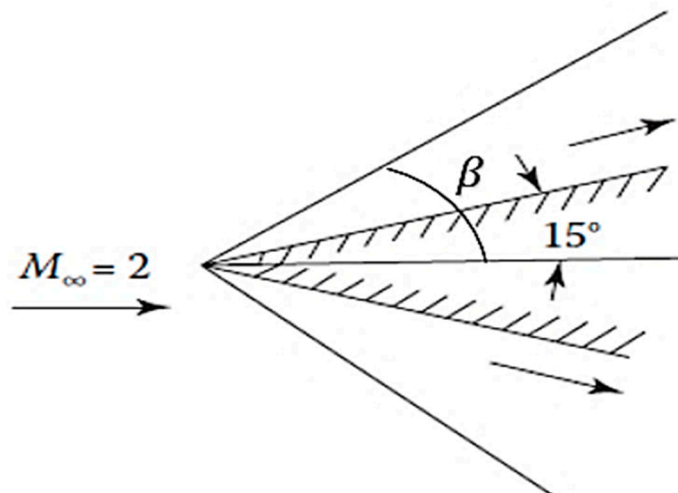


**Figure 1.** Supersonic flow over a wedge angle.

This project, rooted in the realm of compressible flow theory, undertakes a systematic exploration of the flow dynamics surrounding this iconic scenario. It combines theoretical expectations with computational accuracy by using the Steger–Warming flux vector splitting (FVS) method [10–12], an established numerical technique distinguished for its efficiency in capturing the subtlety of shock wave dynamics and the behavior of the complex flow.

To anchor this study, it was restricted to initial conditions that reflect sea level standards, a standard reference point for a multitude of aerospace and aerodynamic endeavors. Here, at this reference point, the pressure holds steady at 101 kPa, the density stands at  $1.22 \text{ kg/m}^3$ , and the temperature remains at 288 K [13]. These initial conditions form the foundation upon which the exploration of the supersonic flow–wedge interaction can be built.

The core objective of this research lies in the comparative analysis between the theoretical underpinnings of compressible flow theory and the numerical outcomes produced by the Steger–Warming FVS method [14,15]. Through this combination, this paper aims to uncover the intricacies of the flow field, delve into the shock wave structure, and dissect the alterations in flow properties arising from the supersonic–wedge encounter. In the sections that follow, this study delves into the mathematical formulation that underlies this investigation, details the numerical methodology, and presents the findings, culminating in a comprehensive assessment of the insights gained from this study. This project advances our understanding of supersonic flow over wedges and paves the way for improved numerical tools in the domain of high-speed aerodynamics, specifically aerospace engineering.

## 2. Methodology

In this section, the results are divided into two approaches. The first part is the theoretical analysis. The second part is the numerical analysis. Then, the differences between them are investigated.

### 2.1. Theoretical Analysis

One of the project’s goals was to conduct a comparative analysis between theoretical and numerical results. As a result, the compressible fluid theory computations were performed initially. To facilitate this, the  $\theta - \beta - M$  chart, as illustrated in Figure 2, was

utilized for the evaluation of the oblique shock angle ( $\beta$ ) and the following compressible fluid flow equations [13].

$$M_{n1} = M_1 \sin \beta \tag{1}$$

$$\frac{\rho_2}{\rho_1} = \frac{(\gamma + 1)M_{n1}^2}{(\gamma - 1)M_{n1}^2 + 2} \tag{2}$$

$$\frac{p_2}{p_1} = 1 + \frac{2\gamma}{\gamma + 1} (M_{n1}^2 - 1) \tag{3}$$

$$\frac{T_2}{T_1} = \frac{p_2}{p_1} \frac{\rho_1}{\rho_2} \tag{4}$$

$$M_{n2}^2 = \frac{M_{n1}^2 + [2/(\gamma - 1)]}{[2\gamma/(\gamma - 1)]M_{n1}^2 - 1} \tag{5}$$

$$M_2 = \frac{M_{n2}}{\sin(\beta - \theta)} \tag{6}$$

$$v_2 = M_2(\gamma RT_2)^{\frac{1}{2}} \tag{7}$$

where:

- $\beta$  = wave angle
- P = pressure
- $\theta$  = wedge angle
- $\rho$  = mass density
- M = Mach number
- M = Mach number
- $\gamma$  = ratio of specific heat
- T = temperature

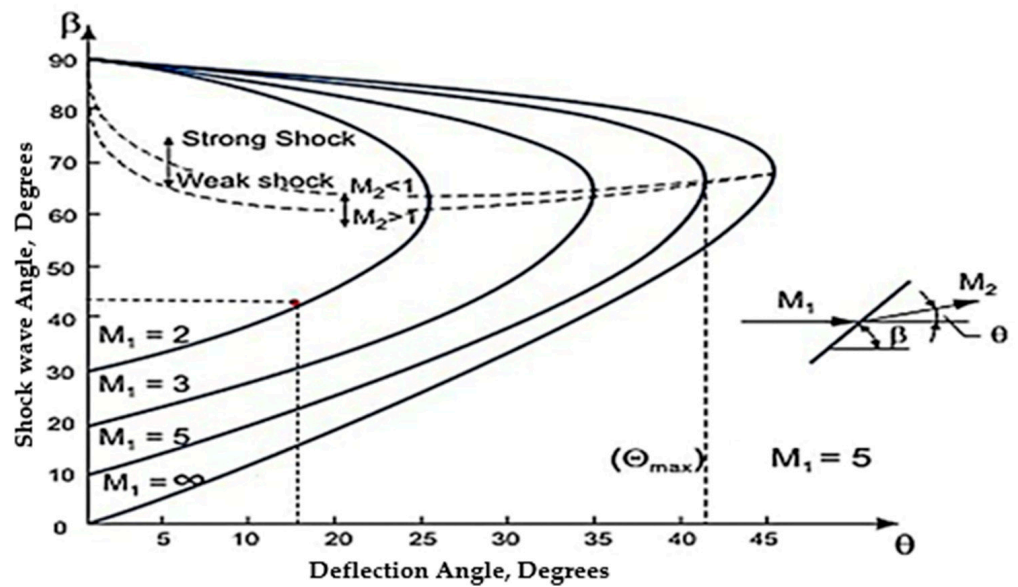


Figure 2.  $\theta - \beta - M$  chart [13].

By solving the above formulas, the theoretical analysis results were obtained and are elaborated in Table 1.

**Table 1.** The calculated theoretical results.

The Downstream Parameters	Theoretical Results
Oblique Shock Angle ( $\beta$ )	45.38°
Mach Number ( $M_2$ )	1.44
Pressure ( $p_2$ ) (kPa)	220.7
Density ( $\rho_2$ ) (kg/m <sup>3</sup> )	2.1
Temperature (K)	365.2
Velocity ( $v_2$ ) (km/h)	1985.76

2.2. Numerical Analysis

Steger–Warming flux vector splitting was utilized throughout this project to solve the two-dimensional Euler equations for supersonic flow over a wedge. On the basis of the laws of conservation of mass, momentum, and energy, 2D Euler equations were developed. The two-dimensional Euler equations’ mathematical representations are demonstrated [11,15–17]:

$$\frac{\partial Q}{\partial t} + \frac{\partial F}{\partial x} + \frac{\partial G}{\partial y} = 0 \tag{8}$$

$$\begin{aligned} \mathbf{F}_{i+\frac{1}{2}} &= \mathbf{F}_i^+ + \mathbf{F}_{i+1}^- = (\mathbf{A}^+ \cdot \mathbf{Q})_i + (\mathbf{A}^- \cdot \mathbf{Q})_{i+1} \\ &= \frac{1}{2}(\mathbf{F}_i + \mathbf{F}_{i+1}) + \frac{1}{2}(|\mathbf{A}|_i \cdot \mathbf{Q}_i - |\mathbf{A}|_{i+1} \cdot \mathbf{Q}_{i+1}) \\ \mathbf{G}_{j+\frac{1}{2}} &= \mathbf{G}_j^+ + \mathbf{G}_{j+1}^- = (\mathbf{B}^+ \cdot \mathbf{Q})_j + (\mathbf{B}^- \cdot \mathbf{Q})_{j+1} \\ &= \frac{1}{2}(\mathbf{G}_j + \mathbf{G}_{j+1}) + \frac{1}{2}(|\mathbf{B}|_j \cdot \mathbf{Q}_j - |\mathbf{B}|_{j+1} \cdot \mathbf{Q}_{j+1}) \end{aligned} \tag{9}$$

$$\mathbf{Q} \equiv \begin{bmatrix} \rho \\ \rho u \\ \rho v \\ \rho E \end{bmatrix} \quad \mathbf{F} \equiv \begin{bmatrix} \rho u \\ \rho u^2 + p \\ \rho uv \\ \rho Eu + pu \end{bmatrix} \quad \mathbf{G} \equiv \begin{bmatrix} \rho v \\ \rho vu \\ \rho v^2 + p \\ \rho Ev + pv \end{bmatrix} \tag{10}$$

where the state variable is represented in algebraic vector form, as shown in Equation (11):

$$\mathbf{Q} = \begin{bmatrix} \rho \\ \rho u \\ \rho v \\ \rho E \end{bmatrix} = \begin{bmatrix} q_1 \\ q_2 \\ q_3 \\ q_4 \end{bmatrix} \quad \mathbf{F} = \begin{bmatrix} q_2 \\ \frac{q_2^2}{q_1} + p \\ \frac{q_2 q_3}{q_1} \\ \frac{q_2 q_4}{q_1} + p \frac{q_3}{q_1} \end{bmatrix} \quad \mathbf{G} = \begin{bmatrix} q_3 \\ \frac{q_3 q_2}{q_1} \\ \frac{q_3^2}{q_1} + p \\ \frac{q_3 q_4}{q_1} + p \frac{q_3}{q_1} \end{bmatrix} \tag{11}$$

Here, two additional equations (energy equations) were integrated. These are:

$$E = e_{\text{int}} + \frac{1}{2}(u^2 + v^2) \tag{12}$$

$$e_{\text{int}} = \frac{p}{\rho(\gamma - 1)} \tag{13}$$

where:

$A$  = flux Jacobin matrix in X-direction

$B$  = flux Jacobin matrix in Y-direction

$u$  = X-component of velocity

$v$  = Y-component of the velocity

$Q$  = state vector

$F$  = flux vector in X-direction

$G$  = flux vector in Y-direction

$E$  = total internal energy

$e$  = internal energy per unit mass

To proceed, two flux Jacobian matrices were created, namely [18]

$$[A] = \frac{\partial F}{\partial Q} \quad \text{and} \quad [B] = \frac{\partial G}{\partial Q} \tag{14}$$

Therefore, the Equation (8) can be rewritten as follows, and the modified shock wave is depicted in Figure 3:

$$\frac{\partial Q}{\partial t} + [A] \frac{\partial F}{\partial Q} + [B] \frac{\partial G}{\partial Q} = 0 \tag{15}$$

where:

$$A \equiv \begin{bmatrix} 0 & 1 & 0 & 0 \\ \frac{1}{2}(\gamma - 1)(u^2 + v^2) - u^2 & u(3 - \gamma) & (1 - \gamma)v & \gamma - 1 \\ -uv & v & u & 0 \\ (\gamma - 1)(u^2 + v^2)u - \gamma Eu & \gamma E - (\gamma - 1)\left(\frac{3}{2}u^2 + \frac{1}{2}v^2\right) & (1 - \gamma)uv & \gamma u \end{bmatrix} \tag{16}$$

$$B \equiv \begin{bmatrix} 0 & 0 & 1 & 0 \\ -uv & v & u & 0 \\ \frac{1}{2}(\gamma - 1)(v^2 + u^2) - v^2 & (1 - \gamma)u & (3 - \gamma)v & \gamma - 1 \\ (\gamma - 1)(u^2 + v^2)v - \gamma Ev & (1 - \gamma)uv & \gamma E - (\gamma - 1)\left(\frac{1}{2}u^2 + \frac{3}{2}v^2\right) & \gamma \end{bmatrix} \tag{17}$$

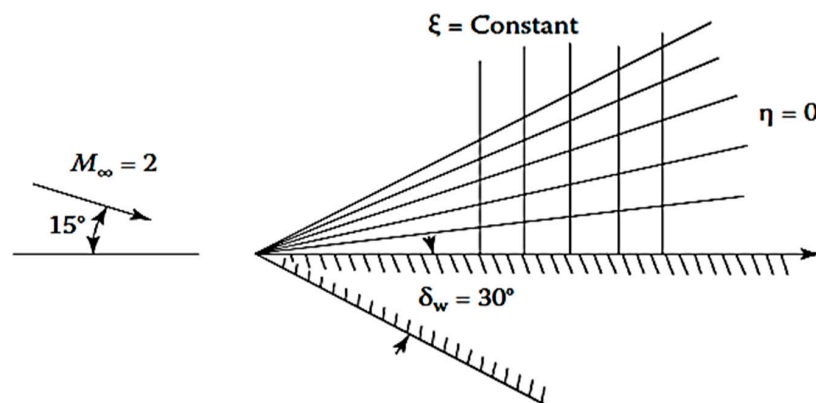


Figure 3. Wedge with a modified shock layer.

Now, the Steger–Warming flux vector splitting (FVS) scheme can be employed. This numerical procedure was developed by Joseph Steger and R.F. Warming (1981) [10], and it was designed to partition the flux into non-negative and non-positive components. Each of these components is associated with the signal propagation direction, a characteristic derived from the scheme’s homogeneity property [19]. Eventually, the accuracy of this scheme is considered first-order in both time and space, and its stability condition is defined by [16]:

$$\Delta t = \frac{CFL}{\left[ \frac{|u|+c}{\Delta x} + \frac{|v|+c}{\Delta y} \right]} \tag{18}$$

where CFL = Courant Fredrick Lewy.

An essential aspect that should be elaborated on deeply is the utilization of the finite volume method, which was selected as the computational approach to obtain the necessary results. Moreover, this scheme aligns with the partial differential equation through the application of the Taylor series [15]. Lastly, the hyperbolic type is the classification of this partial differential equation (PDE).

The downstream flow properties were determined throughout the numerical solution, including oblique shock angle ( $\beta$ ), Mach number, mass density, and pressure. Furthermore,

the research involved the computation of absolute differences in pressure and density between grid points, as clearly illustrated in the obtained results.

The left and top sides of the geometry were fixed using the boundary conditions of the geometry and Equation (19) for the bottom side, as represented in Figure 4, where ( $v = 0$ ) and the flux of the x vector ( $F$ ) is equal to the state vector ( $Q$ ) on the right (i.e.,  $F = Q$ ).

$$F \equiv \begin{bmatrix} 0 \\ p \\ 0 \\ 0 \end{bmatrix} \qquad G \equiv \begin{bmatrix} 0 \\ 0 \\ p \\ 0 \end{bmatrix} \qquad (19)$$

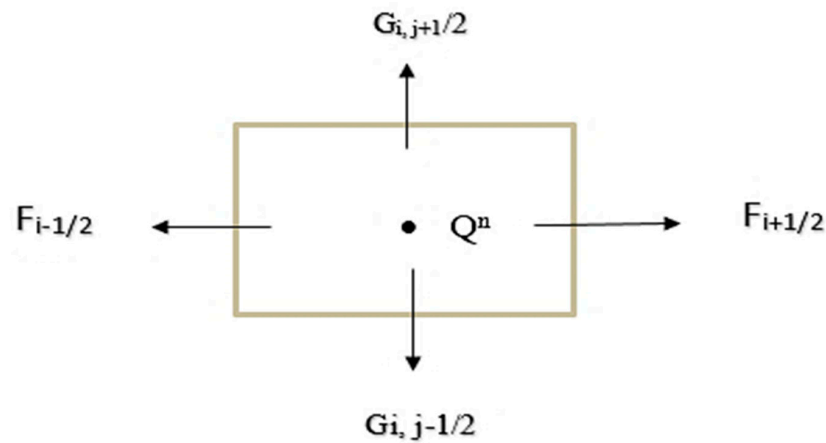


Figure 4. Steger–Warming boundary condition (B.C.).

### 3. Results and Discussion

In this section, all figures and tables belonging to the numerical solution are demonstrated below (Figures 5–9 and Table 2):

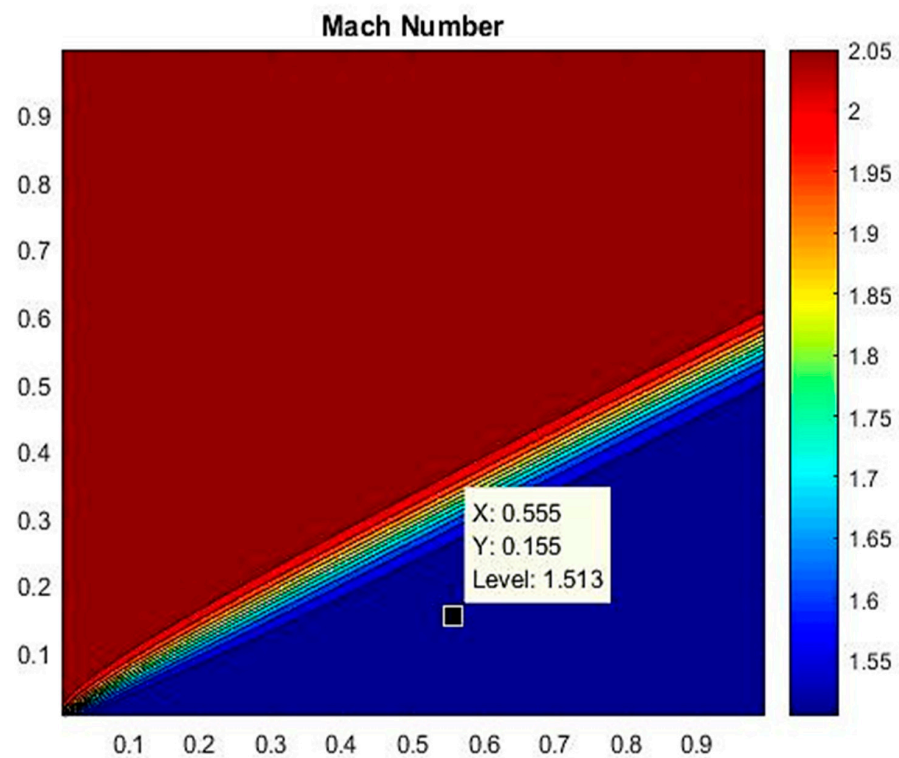


Figure 5. Oblique shock angle ( $\beta$ ) on a half-angle wedge.

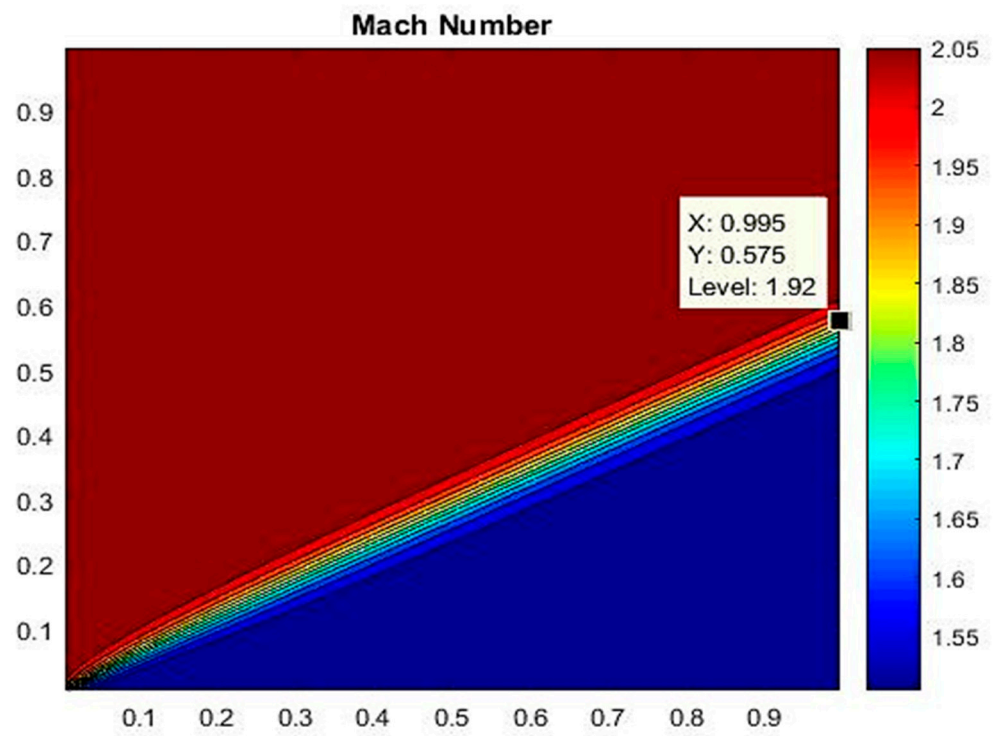


Figure 6. The Mach number behind the Oblique Shock wave on a half-wedge angle.

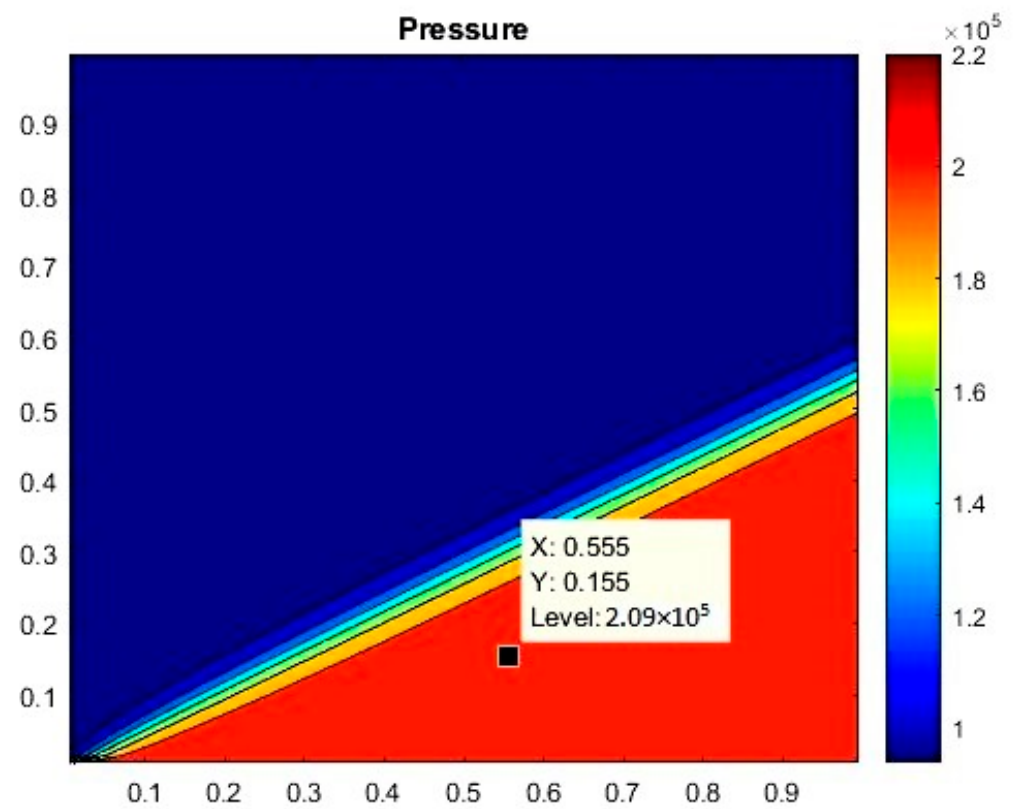


Figure 7. The pressure behind the oblique shock wave on a half-wedge angle.

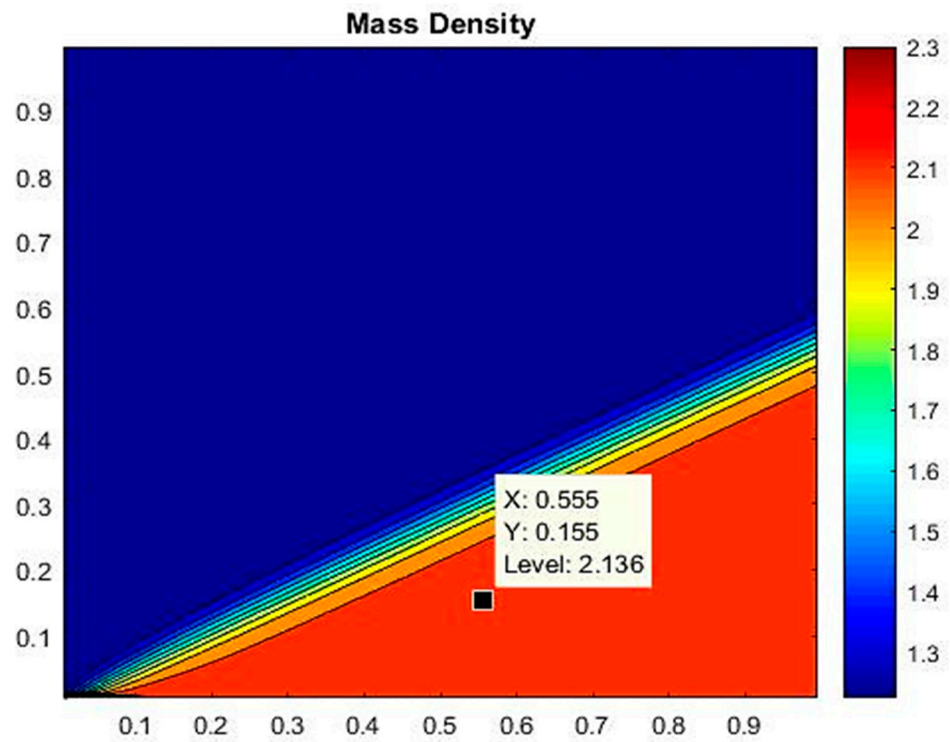


Figure 8. The mass density behind the oblique shock wave on a half-wedge angle.

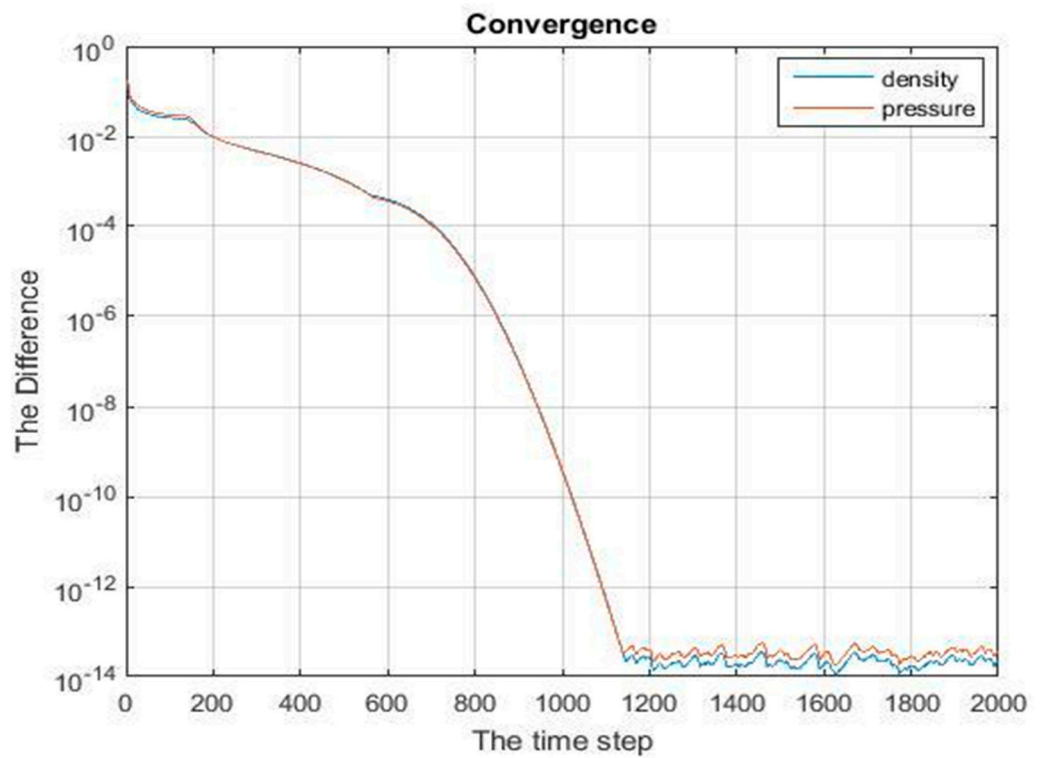


Figure 9. The absolute difference of pressure and density between (n) and (n + 1).

**Table 2.** Theoretical results, numerical results, and error percent.

Parameters	Theoretical Results	Numerical Results	Error Percent (%)
Upstream Mach No.	2.0	2.0	-
Mach Number	1.44	1.513	4.82
Pressure (kPa)	220.7	209	5.3
Density (kg/m <sup>3</sup> )	2.11	2.136	1.2
Oblique Shock Angle ( $\beta$ )	45.38°	45.023°	0.786

#### 4. Discussion

The comprehensive exploration of supersonic flow over the wedge yielded a wealth of numerical parameters, offering profound insights into the intricacies of this complex phenomenon. Among the pivotal parameters extracted from the computational framework was the wave angle ( $\beta$ ), as depicted in Figure 5. In addition, the numerical results unveiled critical metrics—the Mach number, mass density, and pressure downstream of the oblique shock wave ( $\beta$ )—meticulously presented in Figures 6–8.

The characteristic of this investigation resides in the scrupulous comparison between theoretical predictions and numerical results, a process conducted with meticulous precision. The crucible of this evaluation is marked by the selection of a strategically positioned point ( $X = 0.555$  and  $Y = 0.155$ ) behind the oblique shock wave, rendering the assessment insightful and exacting, as succinctly tabulated in Table 2.

It is essential to clarify that the  $X$  and  $Y$  coordinates presented in MATLAB Figures 5–8 represent dimensionless scale coordinates rather than physical units. Moreover, these coordinates serve as relative positions within the plotted data rather than absolute measurements in a specific unit.

A discerning examination of the comparative analysis reveals a confluence of the numerical outcomes with theoretical expectations. Evidently, the disparities, characterized by insignificant error percentages, stand as proof of the adeptness of the numerical approach. Specifically, the error percentages in critical parameters, such as the oblique shock angle ( $\beta$ ) (0.786%), Mach number (4.82%), pressure (5.3%), and mass density (1.2%), barely register as a fractional departure from theoretical calculations. This convergence finds its roots in the diligent execution of a prodigious number of iterations, which is equal to 2000, a factor that underscores the fundamental role of computational resources in bridging the theoretical–numerical divide.

The symbiotic relationship between iterative refinement and convergence is manifested vividly in Figure 9, where a demonstration of the methodical approach emerges. The semiotic narrative unfurls in the form of an unmistakable convergence pattern, marked by an infinitesimal discrepancy thresholding at  $10^{-6}$ . Notably, when the compass of iterations is constrained to a mere 100, the divergence between the exacting theoretical calculations and the numerical outcomes becomes manifest, a compelling validation of the relationship between computational prowess and precision.

In this discerning appraisal, a prescient insight emerges: the pursuit of heightened precision in numerical solutions necessitates not only a greater allocation of temporal resources but also the embrace of advanced computational substructures. The imperative of these enhancements becomes apparent as this study navigates the delicate balance between computational intensity and accuracy, charting a course toward the realization of more efficient, high-speed aircraft design and performance.

#### *Validation and Comparative Assessment*

In direct comparison with Murat Bakırcı’s paper titled “A Numerical Algorithm to Solve Supersonic Flow over a Wedge-Shaped Airfoil”, the present study establishes a novel and rigorous approach for the numerical investigation of supersonic flow over a wedge exploitation the Steger–Warming flux vector splitting (FVS) scheme. However, Bakırcı’s work focused on a MacCormack predictor–corrector approach, whereas the present study har-

nessed the strength of the Steger–Warming FVS scheme, a numerical technique celebrated for its accuracy and stability in capturing the behavior of complex flow phenomena.

Simultaneously, the two studies share common foundational elements, using a wedge angle of  $15^\circ$  and a Mach number of 2 to ensure a consistent baseline for comparison. Nevertheless, when evaluating the results, the divergence in numerical solution schemes becomes apparent. Furthermore, Bakırcı observed some issues with unbounded flow velocities which necessitate correction through synthetic dissipation, highlighting the challenges associated with the MacCormack approach.

By contrast, this article demonstrates the effectiveness of the Steger–Warming FVS numerical method implemented by a MATLAB code. The numerical results exhibited remarkable convergence and accuracy, overcoming the challenges encountered in other schemes. The extensive configuration (validation process) involved theoretical analysis, ensuring that critical parameters such as Mach numbers and oblique shock wave angles were accurate. This validation was not only performed internally but also compared with theoretical expectations, and it improved the reliability of the findings.

Furthermore, while Bakırcı validates the results using ANSYS Fluent, MATLAB code (Appendix A) was used in this study, providing a unique advantage. MATLAB code not only captures shock waves accurately but also facilitates a deeper understanding through theoretical analysis. The list of critical parameters in Table 2 and the visual illustrations in Figures 5–8 demonstrate the effectiveness of the code in predicting the main flow characteristics [20].

## 5. Conclusions

A comprehensive investigation and study of supersonic flow dynamics on a wedge using a complex Steger–Warming flux vector splitting (FVS) scheme is an important contribution to the growing field of aerospace engineering. This inquiry was underpinned by a precise selection of initial conditions, enabling a more accurate evaluation of properties emergent beyond the oblique shock, a naturally characteristic phenomenon engendered by the exertion of supersonic flow over a region at the compression angle. Within this rigorous arrangement, delineated by an upstream Mach number of 2.0 and a wedge angle ( $\theta$ ) of  $15^\circ$ , the theoretical structure leaned significantly on the principles of compressible fluid theory, an academically revered foundation in aerodynamic analysis or study.

By contrast, the numerical aspect of this investigation utilized the powerful Steger–Warming technique, demonstrating computational superiority in the outcome estimation. In this numerical analysis, the mandatory finite volume method took center stage, effectively approximating solutions to the challenging 2–D Euler equations. The key to the method's effectiveness was its precise flux partitioning, a complex numerical technique that balanced theoretical postulates with computing accuracy.

Within the comparative analysis, there was a remarkable convergence between the statistical and theoretical aspects, although not without a noticeable percentage of error. This delicate divergence assumed prominence at an appropriately selected reference point ( $X = 0.555$  and  $Y = 0.155$ ) behind the oblique shock wave. These fractional anomalies, although undetectable, registered their presence under important parameters, including the obvious oblique impact angle ( $\beta$ ) (0.786%), Mach number (4.82%), mass density (1.2%), and pressure (5.3%).

The iterative underpinning of numerical precision resided at the forefront of this inquiry, where the cumulative tally of 2000 iterations, underpinned by a convergence criterion of  $10^{-6}$ , fortified the bridge between theoretical and numerical accuracy. This expansive iterative endeavor elucidates the quintessential role played by computational resources, highlighting a salient need for advanced processing substructures to further reduce the theoretical–numerical divide.

This research lends irrefutable credence to the symbiotic nexus between academic rigor and practical application. Its ramifications extend beyond the confines of theoretical discourse, transcending into the real-world arena of high-speed aircraft design and per-

formance. Here, the vision of more efficient, high-speed aircraft components crystallizes, forging a path toward aerospace excellence, where the convergence of academic rigor and practicality engenders cutting-edge advancements in aerospace engineering.

**Author Contributions:** Conceptualization, H.H.A.; Methodology, H.H.A.; Original draft preparation, H.H.A. and H.A.K.S.; Validation, H.H.A., Visualization, H.H.A. and H.A.K.S.; Resources, H.H.A., H.A.K.S. and M.W.; Supervision, M.W. All authors have read and agreed to the published version of the manuscript.

**Funding:** This research received no external funding.

**Data Availability Statement:** Data are contained within the article.

**Conflicts of Interest:** The authors declare that they have no known competing financial interests or personal relationships that could have appeared to influence the work reported in this paper.

## Appendix A

A MATLAB algorithm for solving the 2D supersonic wedge flow governed by the Euler equations was built to supplement the numerical investigations presented in this article. In computational fluid dynamics, the Steger–Warming flux vector splitting (FVS) approach is a robust numerical scheme widely utilized in this implementation. The MATLAB code serves as a platform for simulating the behavior of the flow field under various conditions and a tool for simulating the complex interactions of supersonic flow over a wedge. The code encapsulates the fundamental equations governing compressible flow, allowing for the accurate representation of shock waves and other critical phenomena inherent to supersonic aerodynamics. Practitioners and researchers interested in further exploring and validating the results presented in this scientific article are encouraged to refer to the provided MATLAB code in the Appendix A. The code includes detailed comments to facilitate comprehension and extension for future studies.

```
% Numerical Solution of Euler Equations for 2D Supersonic Wedge
Flow
with Steger Warming Method (Basic Equation):
%
%  $F_{\{j+1/2\}} = 0.5*(F_{\{j+1\}} + F_{\{j\}}) - 0.5*(A_{\{j+1\}} * Q_{\{j+1\}} -$ 
 $A_{\{j\}}*Q_{\{j\}})$ 
%
%  $G_{\{j+1/2\}} = 0.5*(G_{\{j+1\}} + G_{\{j\}}) - 0.5*(B_{\{j+1\}} * Q_{\{j+1\}} -$ 
 $B_{\{j\}}*Q_{\{j\}})$ 
%
%  $Q^{\{n+1\}}_j = Q_j - (Dt/h)*(F^*_j+1/2 - F^*_j-1/2)$ 
%
%
clear all; clc;

% Set the constants
Nmx = 100; % Number of cells in horizontal dimension
Nmy = 100; % Number of cells in vertical dimension
Ntm = 2000; % Number of time steps
```

```

length = 1.0; % Space domain
h = length/Nmx; % Space interval

% ----- Initial Conditions -----
*
Gamma = 1.4; GM1 = Gamma - 1;

p_0 = 101325; T_0 = 288.15; RGAS = 287.0; rho_0 = p_0/T_0/RGAS;
M_0 = 2.0; % Freestream Mach number
theta = 15.0 * pi/180; % Wedge half-angle = turning angle
V_0 = sqrt(Gamma*p_0/rho_0)*M_0; % Freestream flow speed
u = V_0 * cos(theta);
v = -V_0 * sin(theta);
E = 0.5*u^2 + p_0/rho_0/GM1;
Q(1)= rho_0 ; Q(2)= rho_0 * u ; Q(3)= rho_0 * V_0 ; Q(4)= rho_0 *
E;
% Initialize the arrays

% ----- Boundary Conditions for Interface Half-Fluxes -----
----- *

% Left side is supersonic inflow, remains fixed at freestream
conditions
% Right side is supersonic outflow, extrapolate from interior
cell
% ----- Set up arrays & post-process for display -----
----- *

pressure = zeros(Nmx,Nmy); density = zeros(Nmx,Nmy);
temperature=zeros(Nmx,Nmy);
velocity_x = zeros(Nmx,Nmy); velocity_y = zeros(Nmx,Nmy);
entropy = zeros(Nmx,Nmy); machNum = zeros(Nmx,Nmy);

for i=1:Nmx
for j=1:Nmy
density(j,i) = Qn(j,i,1);
else
u = 0; v = 0;
end
velocity_x(j,i) = u;
velocity_y(j,i) = v;
pressure(j,i) = (Qn(j,i,4) - 0.5*Qn(j,i,2)*u - 0.5*Qn(j,i,3)*v )
* GM1;
Vel = sqrt(u^2 + v^2);

```

```
if Qn(j,i,1) > 0
c = sqrt( Gamma * pressure(j,i) / Qn(j,i,1) );
machNum(j,i) = Vel/c;
else
c = 0; machNum(j,i) = 0;
end

entropy(j,i) = density(j,i)*( log(pressure(j,i)/p_0)/GM1 -
Gamma*log(density(j,i)/rho_0)/GM1 );
end
end

uS = velocity_x .* entropy;
vS = velocity_y .* entropy;

S_gen = divergence(xc,yc,uS,vS);

figure(1)
contourf(xc,yc,abs(pressure));
colormap(jet)
title('Pressure');
colorbar

figure(2)
contourf(xc,yc,abs(density));
colormap(jet)
title('Mass Density');
colorbar

figure(3)
contourf(xc,yc,abs(machNum));
colormap(jet)
title('Mach Number');
colorbar

figure(4)
contourf(xc,yc,abs(entropy));
colormap(jet)
title('Entropy');
colorbar
```

```

figure(5)
contourf(xc,yc, abs(sqrt(velocity_x.^2+velocity_y.^2)));
colormap(jet)
title('Velocity Field');
hold on;
quiver(xc,yc,abs(velocity_x), abs(velocity_y));
hold off;
colorbar

```

```

figure(6)
contourf(xc,yc,abs(S_gen));
colormap(jet)
title('Entropy Generation');
colorbar

```

```

figure(7)
semilogy(max_rho)
hold on
semilogy(max_press)
hold off
xlabel('The time step')
ylabel('The Difference')
legend('density', 'pressure', 'Location', 'northwest', 2);
title('Convergence')
grid
%end

```

## References

1. Abada, H.H. Turboelectric Distributed Propulsion System for NASA Next Turboelectric Distributed Propulsion System for NASA Next Generation Aircraft Generation Aircraft. Master's Thesis, Wright State University, Dayton, OH, USA, 2017. Available online: [https://corescholar.libraries.wright.edu/etd\\_all](https://corescholar.libraries.wright.edu/etd_all) (accessed on 9 October 2023).
2. Newman, P.A.; Allison, D.O. *An Annotated Bibliography on Transonic Flow Theory*; National Aeronautics and Space Administration: Washington, DC, USA, 1971; p. 20546. Available online: <https://ntrs.nasa.gov/api/citations> (accessed on 9 May 2023).
3. Liu, Y.-S.; Wu, D.; Wang, J.-P. Structure of an oblique detonation wave induced by a wedge. *Shock. Waves* **2015**, *26*, 161–168. [[CrossRef](#)]
4. Bagabir, A.; Drikakis, D. Numerical experiments using high-resolution schemes for unsteady, inviscid, compressible flows. *Comput. Methods Appl. Mech. Eng.* **2004**, *193*, 4675–4705. [[CrossRef](#)]
5. Özgün, M. Analysis of Hypersonic Flow Using Three Dimensional Navier-Stokes Equations. Master's Thesis, Graduate School of Natural and Applied Sciences of Middle East Technical University, Ankara, Turkey, 2016.
6. Eraslan, E. Implementation of Different Flux Evaluation Schemes into a Two-Dimensional Euler Solver. Master's Thesis, Middle East Technical University, Ankara, Turkey, 2006.
7. Hu, J. A Computational Fluid Dynamics Analysis of Shock Wave-Boundary Layer Interactions. Master's Thesis, Auburn University, Auburn, Alabama, 2018. Available online: <https://etd.auburn.edu/handle/10415/6320> (accessed on 15 January 2024).
8. Aabid, A.; Khan, S.A.; Baig, M. A Critical Review of Supersonic Flow Control for High-Speed Applications. *Appl. Sci.* **2021**, *11*, 6899. [[CrossRef](#)]
9. Tu, G.; Zhao, X.; Mao, M.; Chen, J.; Deng, X.; Liu, H. Evaluation of Euler fluxes by a high-order CFD scheme: Shock instability. *Int. J. Comput. Fluid Dyn.* **2014**, *28*, 171–186. [[CrossRef](#)]
10. Steger, J.L.; Warming, R. Flux vector splitting of the inviscid gasdynamic equations with application to finite-difference methods. *J. Comput. Phys.* **1981**, *40*, 263–293. [[CrossRef](#)]

11. Nguyen, B.H.; Le, G.S. Comparative study of numerical schemes for strong shock simulation using the Euler equations. *Sci. Technol. Dev. J.* **2015**, *18*, 73–88. [[CrossRef](#)]
12. Qu, F.; Sun, D.; Liu, Q.; Bai, J. A Review of Riemann Solvers for Hypersonic Flows. *Arch. Comput. Methods Eng.* **2022**, *29*, 1771–1800. [[CrossRef](#)]
13. Anderson, J.D. *Modern Compressible Flow with Historical Perspective*, 3rd ed.; McGraw-Hill Series in Aeronautical and Aerospace Engineering; New York, NY, USA, 1990.
14. Tchien, G.; Fogang, F.; Burtschell, Y.; Wofo, P. A hybrid numerical method and its application to inviscid compressible flow problems. *Comput. Phys. Commun.* **2014**, *185*, 479–488. [[CrossRef](#)]
15. Kriel, A. A flux splitting method for the Euler equations. *J. Comput. Phys.* **2014**, *278*, 326–347. [[CrossRef](#)]
16. Tannehill, J.C.; Anderson, D.A.; Pletcher, R.H. *Computational Fluid Mechanics and Heat Transfer*, 2nd ed.; Taylor and Francis: New York, NY, USA, 1997; Volume 8.
17. Witherden, F.D.; Jameson, A. On the spectrum of the Steger-Warming flux-vector splitting scheme. *Int. J. Numer. Methods Fluids* **2018**, *87*, 601–606. [[CrossRef](#)]
18. Garg, N.K.; Maruthi, N.; Rao, S.R.; Sekhar, M. Use of Jordan forms for convection-pressure split Euler solvers. *J. Comput. Phys.* **2020**, *407*, 109258. [[CrossRef](#)]
19. Tannehill, J.C.; Anderson, D.A.; Pletcher, R.H. *Computational Fluid Mechanics and Heat Transfer*, 3rd ed.; Taylor and Francis: New York, NY, USA, 2012.
20. Bakirci, M. A Numerical Algorithm to Solve Supersonic Flow over a Wedge Shaped Airfoil. *Eur. J. Sci. Technol.* **2020**, *18*, 934–942. [[CrossRef](#)]

**Disclaimer/Publisher’s Note:** The statements, opinions and data contained in all publications are solely those of the individual author(s) and contributor(s) and not of MDPI and/or the editor(s). MDPI and/or the editor(s) disclaim responsibility for any injury to people or property resulting from any ideas, methods, instructions or products referred to in the content.